Cell sprouting and colonization in platelet lysate-functionalized hydrogels for peri-implant bone regeneration

Master thesis by

Sidra Hubous and Sara Ibrahim

Supervisor: Hanna Tiainen

Department of Biomaterials
Institute of Clinical Dentistry
University of Oslo
2023

Table of contents

Abstract

Peri-implantitis, an inflammatory condition affecting dental implants, can pose challenges both in terms of efficacy and long-term success and in some cases lead to the loss of dental implants due to loss of surrounding bone. No optimal treatment approach is yet found as there is still limitations in promoting bone repair and regeneration. New strategies are therefore needed to facilitate bone regeneration and to reverse the loss of supportive peri-implantitis tissue.

There is an increasing interest on investigating therapeutic treatments that can promote cell sprouting and colonization of biomaterials. One such approach is injectable calcium phosphate-hydrogel composites modified with platelet lysate (PL). These composites can replicate the properties found in bone and give an optimal microenvironment which can promote cell recruitment and initiate bone formation. PL can deliver growth factors, chemo-attractants, calcium and phosphate ions which are vital for the regenerative process. Hereby we studied the effect of the concentration of platelet lysate proteins encapsulated in polyethylene glycol (PEG) hydrogels on cell colonization of the hydrogel matrix. Our aim was to investigate to investigate the effect of the concentration of platelet lysate proteins encapsulated in polyethylene glycol (PEG) hydrogels on cell colonization of the hydrogel matrix. For this we used hydrogels with different PL concentrations. Results showed that cell colonization is visible with higher PL concentration, however the RGD peptide is essential. The findings suggest that the combination of PL and RGD in hydrogels have the potential to be an effective assist in cell migration. However, it is difficult to give any firm conclusions, further investigations should be done.

Acknowledgements

We would like to thank our supervisor professor Hanna Tiainen for her guidance and support throughout the duration of this master project.

We also would like to extend our appreciation to Catherine Anne Heyward for teaching us how to operate and utilize the confocal microscope effectively.

We are also grateful to the Department of Biomaterials and University of Oslo for giving us access to their well-equipped laboratory facilities.

Abbreviations and notations

α-MEM	α-minimum essential media
BCA	Bicinchoninic acid
BSA	Bovine serum albumin
DAPI	4′,6-diamidino-2-phenylindole
CLSM	Confocal laser scanning microscope
ECM	Extracellular matrix
hMSCs	Human mesenchymal stem cells
PB	Phosphate buffer
PBS	Phosphate buffered saline
PDL	Periodontal ligament
PEG	Poly(ethylene glycol)
PFA	Paraformaldehyde
PL	Platelet lysate
PRP	Platelet-rich plasma
RGD	Arginine-glycine-aspartate
TGF	Transforming growth factor

1. Introduction

In the field of dentistry, dental implants have revolutionized the way we can replace missing teeth by giving a long-lasting and effective solution. Compared to the traditional options such as dentures and bridges, dental implants are more comfortable and do not require removal of adjacent teeth structures [1]. They mirror the function and appearance of a natural tooth, allowing patients to speak, chew, smile with confidence and preserve the alveolar bone [2].

However, despite their benefits and high success rates, dental implants can fail due to several factors such as smoking, improper placement of the implants, poor quality of surrounding bone, design failure, poor oral hygiene, uncontrolled diabetes and bacterial infection [3]. The most important factor that leads to implant failure is bacterial infection that causes peri-implantitis [4]. Peri-implantitis is an inflammatory disease that affects the tissue surrounding the inserted dental implants, which can lead to bone loss and eventually implant failure [1, 5]. This disease affects around 13% of the population with dental implants [6]. Compared to inflammation around natural teeth, peri-implantitis is more aggressive and faster which can lead to implant loss faster than natural tooth loss [7].

This type of inflammation is driven mainly by bacterial colonisation. When a newly inserted implant is exposed to the oral cavity, it becomes immediately covered by a protein layer called the salivary pellicle, and is colonised by oral microorganisms, forming a microbial biofilm [8]. This development of an adherent plaque layer on the implant plays an important role in developing peri-implantitis subsequently altering the implant's surface biocompatibility [5].

The main difference between the implant and natural tooth is that the implant joins the bone directly (osseointegration) and the tooth is connected to the adjacent bone via the periodontal ligament (PDL) [9, 10]. Therefore, the implant lacks innervation [11, 12]. Early stage of peri-implantitis is often asymptomatic, meaning that the patient experiences no signs of the infection [13, 14]. This leads to delayed detection of inflammation which requires extensive care and treatment, in most cases with surgical methods [14] .

Treatment methods for peri-implantitis can be divided into non-surgical and surgical. Non-surgical approach includes antiseptic, mechanical debridement and use of

antibiotics. Surgical methods include air powder abrasive, resective and regenerative surgery [15]. However, as of today there is yet no method that can be defined as an optimal treatment to fully resolve the inflammation around the implant [16].

To limit or stop the condition, peri-implantitis is treated using two approaches [17]

1) Resective therapy: the goal is etiologic factor elimination and maintenance of the implant by manual surface cleaning.
2) Regenerative therapy: the goal of which is to reconstruct the lost tissues using different methods (e.g., guided bone regeneration, grafts and scaffolds)

To limit the complete loss of the surrounding tissue and to enable bone regeneration, surgical intervention therapy is recommended for treating peri-implantitis [18]. This includes regenerative therapy which attempts to regenerate bone around the inflammation sites. Hydrogels can offer a potential solution for tissue regeneration due to their biocompatibility, composition and provide a 3D scaffold for cell growth and regeneration. Integrating platelet lysate (PL) with hydrogels can potentially promote cell adhesion [19].

1.1 Role of extracellular matrix (ECM) and hydrogels

ECM was earlier believed to play a passive role and serve like a glue between cells. Recent research revealed that ECM plays an important role in tissue formation and stability [20]. It's a dynamic structure that aid in communication between so called cell-to-cell signaling. This communication is bidirectional, i.e., cells form and receive information from ECM and vice versa [21].

Hydrogels are used to mimic the natural ECM as they can provide the needed structural support for the cells. They can also be tethered with essential chemical components important for cell signaling and cell adhesion [22, 23]. Hydrogels composed of star poly(ethylene glycol) (PEG) macromers crosslinked with cell-cleavable peptides have previously been used as a substitute for natural ECM in vitro [24]. Cells naturally interact with ECM both chemically and physically. The physical communication occurs via transmembranous proteins celled integrins. For biologically inert PED hydrgoels, such communication with cells can only occur after their functionalization [25]. Synthetic arginine-glycine-aspartate (RGD) peptides have been used to functionalize the star PEG arms prior to crosslinking to serve as tethering points for adhesion of cells [24]. It is beneficial to use RGD because it is highly

reproducible, at low cost compared to isolating natural adhesion proteins from tissues or cell cultures. It also very small in size when compared to ECM proteins and less susceptible to degradation. Furthermore, RGD play a major role in cell-to-cell contact, as well as cell differentiation and morphology [26, 27].

1.2 Use of bioactive molecules

Functionalizing the star (PEG) arms with RGD alone is not sufficient to get tissue regeneration started by recruitment of regenerative cells from the surrounding healthy tissues. Bioactive components are highly needed to achieve this, and growth factors are often added to ECM-substitute materials. In this study, platelet lysate (PL) was used as a chemoattractant to enhance cell recruitment and migration within the PEG hydrogel.

1.3 Why PL?

In previous studies, platelet-rich plasma (PRP) has been used to stimulate periodontal tissue regeneration as it contains many growth factors important for tissue regeneration [28]. PRP is produced by multiple centrifugations of an isolated platelet concentrate. When this PRP is lysed either by repetitive freezing and thawing or by ultrasound disruption, a new product called platelet lysate (PL) is formed [29]. Upon processing of PL, growth factors get released and unlike PRP, it needs no activation upon use. These growth factors have insignificant variation which is beneficial when it comes to prediction of the outcome. In addition, PL contains cell adhesion molecules, important for adhesion between cells and ECM. PL is a better product to be used when compared to PRP, as it is easy to store it frozen and thaw on demand [30, 31].

2 Aim

The aim of the study is to investigate the effect of the concentration of platelet lysate proteins encapsulated in polyethylene glycol (PEG) hydrogels on cell colonization of the hydrogel matrix.

2.1 Hypothesis

Based on the research questions introduced above, a general hypothesis for the study was formulated as follows:

Human MSCs encapsulated in PEG hydrogels sprout out from a cell spheroid and colonize the hydrogel matrix faster and more efficiently in hydrogels with higher platelet lysate concentration. The higher the PL concertation, the more effective the cell colonization.

3 Materials and methods

3.1 Hydrogel preparation for protein release

Hydrogels were produced from the polymer vinylsulfone-functionalized 8-arm PEG macromers with a molecular weight of 40 kDa (Jenkem Technology, USA). The macromers were diluted with 100µl of platelet lysate (PL produced by 3Bs at University of Minho, Portugal, as described in [32]) serially diluted in 25 mM phosphate buffer (PB) as shown in Table 1. All hydrogels contained 5 wt% polymer. A cross-linking peptide (Ac-GCRDVPMSMRGGDRCG-NH_2; Pepmic Co, China) was pipetted to the polymer solution to cross-link the macromers into gels. The same cross-linking peptide was used for all hydrogels produced in this study. Two sets of gels were produced for this study: PL-loaded and PL-loaded functionalized with2.5 mM cyclic RGD (Cyclo(RGD(dF)C), AnaSpec, USA). All gels contained 90 vol. % macromers dissolved in PL solution and 10 vol. % of cross-linker solution. In order to form uniform disk-shaped gels, the polymer-cross-linker solution was pipetted between two glass slides (coated with Sigmacote, Sigma-Aldrich) separated using 1 mm spacer. These were moved to be incubated at 37°C for 30 minutes. After incubation, the gels were transferred to Eppendorf tubes filled with 700 µl PBS. For the cell invasion study, 30µl of hydrogels were formed into disks with encapsulated cell spheroids.

Sample	100% PL	75% PL	50% PL	25% PL	10% PL	0% PL
PL stock	100 µl	75 µl	50 µl	25 µl	10 µl	0 µl
25 mM PB	0 µl	25 µl	50 µl	75 µl	90 µl	100 µl

Table 1*: PL solutions. Gels contain 90 vol. % macromers dissolved in PL solution and 10 vol. % of cross-linker solution.*

3.2 BCA analysis

The Pierce BCA Protein Assay Kit (Thermo Scientific, USA) was used to assess the amount of total protein released from the PL-loaded hydrogel disks. The given protocol by the producer was followed. First the BCA working reagent was prepared following the formula given by the kit. Hydrogel disks were stored in microtubes filled with 700µL PBS. Plates were incubated for 30 minutes at 37°C. The liquid around the hydrogels samples were collected at 1, 2, 4, 24, 72 and 168 h. Collected samples were frozen at -20°C until analysis was performed. Total protein was measured at an absorbance

of 562 nm. Data are plotted as mean ± standard deviation for independent samples at each timepoint (n=3).

3.3 Cell culture

In this experiment, human mesenchymal stem cells (hMSCs) obtained from a single donor were purchased from Lonza. hMSCs were cultured at 37°C in a 5% CO_2 incubator using FBS-supplemented α-MEM (Thermo Scientific, USA) containing 50 U/ml penicillin, 50 mg/ml streptomycin, and 2 mM GlutaMAX (Gibco, USA) to maintain the cells in an undifferentiated state. The cells used in this experiment have been previously characterized for their expression of mesenchymal stem cell markers, showing high expression of CD105, CD44, CD166, CD73 and CD90. When the cells became 75% confulent, they were trypsinized for seeding into hydrogels. Experiments were performed at passage 5 after isolation.

3.4 Cell invasion studies

The cell invasion studies were performed by placing the 1×10^4 cells contained in the spheroid into gel disk before its gelation. Spheroids were formed by culturing the hMSCs in non-adherent round-bottomed ultra-low cluster well plates (Corning Inc., USA) for 24 h prior to start of the experiment. When the spheroids were formed, medium was carefully disposed, and a polymer-cross-linker solution was added into the well to encapsulate the spheroid into the solution before its gelation. The hydrogel mixture holding the spheroid was pipetted between two hydrophobic glass slides to produce a hydrogel disk as previously described using hydrogel compositions given in Table 2. The hydrogel disks with spheroids were then placed in a 24-well plate that contained 700 µL PBS. Later on, images of cell spheroids were captured using phase contrast microscopy at 0 h, 24 h, 48 h, 3 d, 7 d, 10 d and 14 d.

	100% PL	**75% PL**	**50% PL**	**0% PL**
cRGD stock	0	0 / 10	0 / 10	10
PL	90	67.5	45	0
25 mM PB	0	22.5 / 12.5	45 / 35	80
XL	10	10	10	10

***Table 1**: Hydrogel compositions used in the experiment; numbers given in µl for 100µl hydrogel solution with 5 wt.% PEG content*.

3.5 Fixation for confocal imaging

At timepoints 48h, 72h, 7d and 14d one gel per group was removed for fixing and staining for confocal microscopy. Cells were fixed with 4% paraformaldehyde (PFA) for 20 min. The PFA was discarded and the hydrogel samples were washed with PBS three times. To get the fluorescent label of the F-actin and cytoskeleton, cells were incubated at room temperature with phalloidin-Alexa Fluor 568 (Invitrogen, USA) 1:400 solution for 1h. The solution was disposed and the samples were washed with PBS three times. To stain the cell nuclei, DAPI (Invitrogen, USA) was used at 1:1000 working dilution. Samples were imaged with a 20×/0.40 HCX PL APO CSon a Leica SP8 confocal laser scanning microscope using 638 nm excitation for phalloidin and 405 nm for DAPI.

4 Results

4.1 BCA analysis

The results from the BCA analysis provides us with information about the protein concentration in the samples. A standard curve for protein concentration was generated using bovine serum albumin (BSA). The known protein concentrations of serial dilutions of BSA were plotted as a function of measured BCA absorbance as shown in Figure 1 to calculate the linear relationship between BCA absorbance and protein concentration. With this formula, we can calculate the unknown concentration of the test samples.

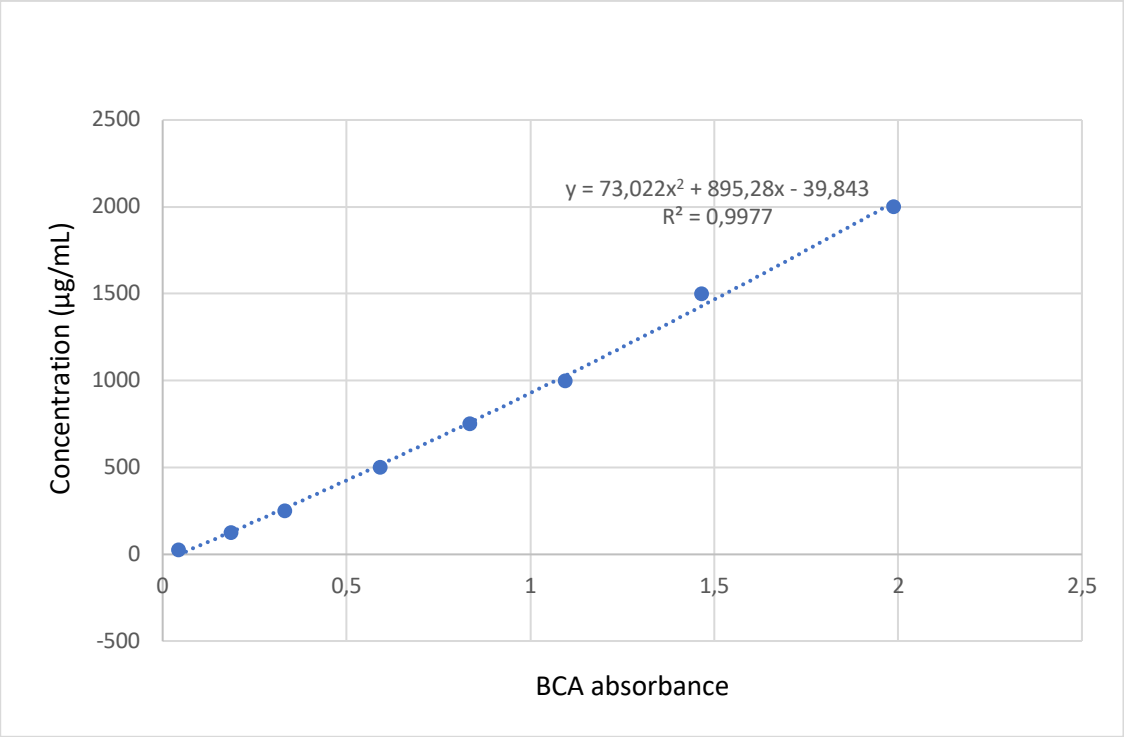

***Figure 1**: BCA analysis. Figure shows the absorbance of known concentrations of serial dilutions of BSA.*

At one hour the most protein release is observed for all PL-loaded hydrogels (Figure 2). The amount of protein release decreases with time. The linear increase of protein concentration released demonstrates the gradual diffusion of proteins from the PL hydrogels without any external flushing necessary.

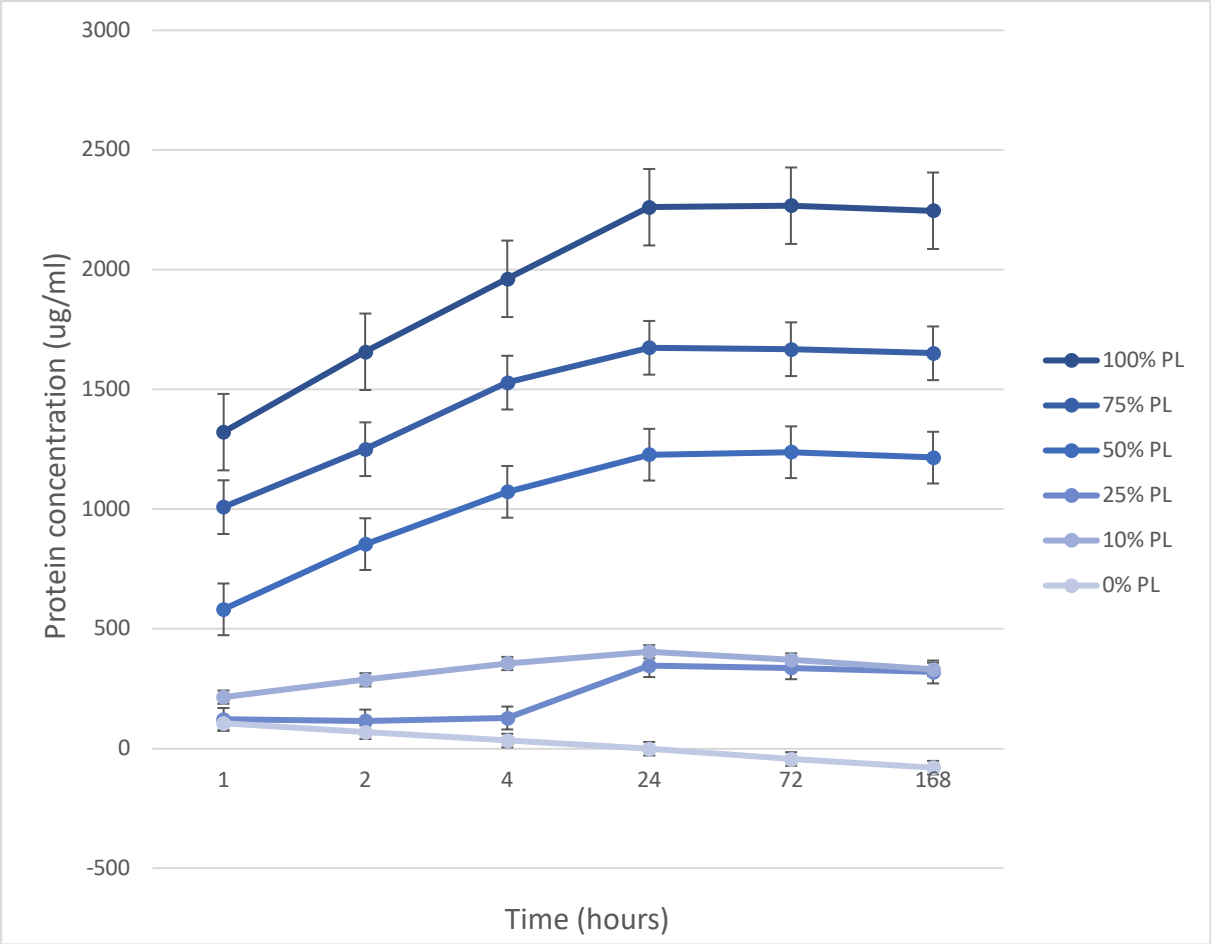

***Figure 2**: Protein release for different PL-loaded hydrogels with different PL concentrations. Protein concentration (y-axis) vs time in hours (x-axis).*

A linear increase is observed until timepoint 24 h for concentrations 100%, 75% and 50%. In other words, the protein concentration released is proportional. At 100% it was calculated that 83% of total protein was released. With the 75% concentration, around 82% of total loaded PL protein was released while 90% of total loaded PL was released with the 50% concentration. The graph begins to flatten with time. This indicates that the percentage of total protein released reaches a maximum at a certain timepoint and proteins are no longer released or are released in too low concentration to be detected by BCA assay. The flattening of the graph is observed earlier for PL solutions with the lower concentrations of 10% and 25%. At 25% it was calculated that 51% of total loaded PL protein was released, while of total loaded PL was released with the 10% concentration.

There is no significant difference in protein release that could be observed at timepoint 1 h between the PL concentration 10% and 25%

4.2 Cell invasion

The capacity of infiltration for hMSC spheroids encapsulated in hydrogels was assessed qualitatively. The assessment is done by taking images of the samples using phase contrast microscope. Figure 3 show the cell invasion for different PL concentrations in chronological order.

In Figure 3 it is observed that 0% PL, shows no signs of cells emerging from the spheroid at the end timepoint 14 days despite the presence of RGD cell-binding ligands in the hydrogels. Similarly in the 100% PL loaded hydrogel sample without RGD functionalization, no signs of cellular motility or any other forms of movement were observed.

Cells encapsulated within RGD-functionalized PL-loaded hydrogels exhibit the most growth and the fastest growth, whereas this was not observed in the corresponding gel groups without RGD. Both hydrogels with 50% PL + RGD and 75% PL + RGD showed visible invasion at day 3 (72 h). The movement of cells from the spheroid increased with time.

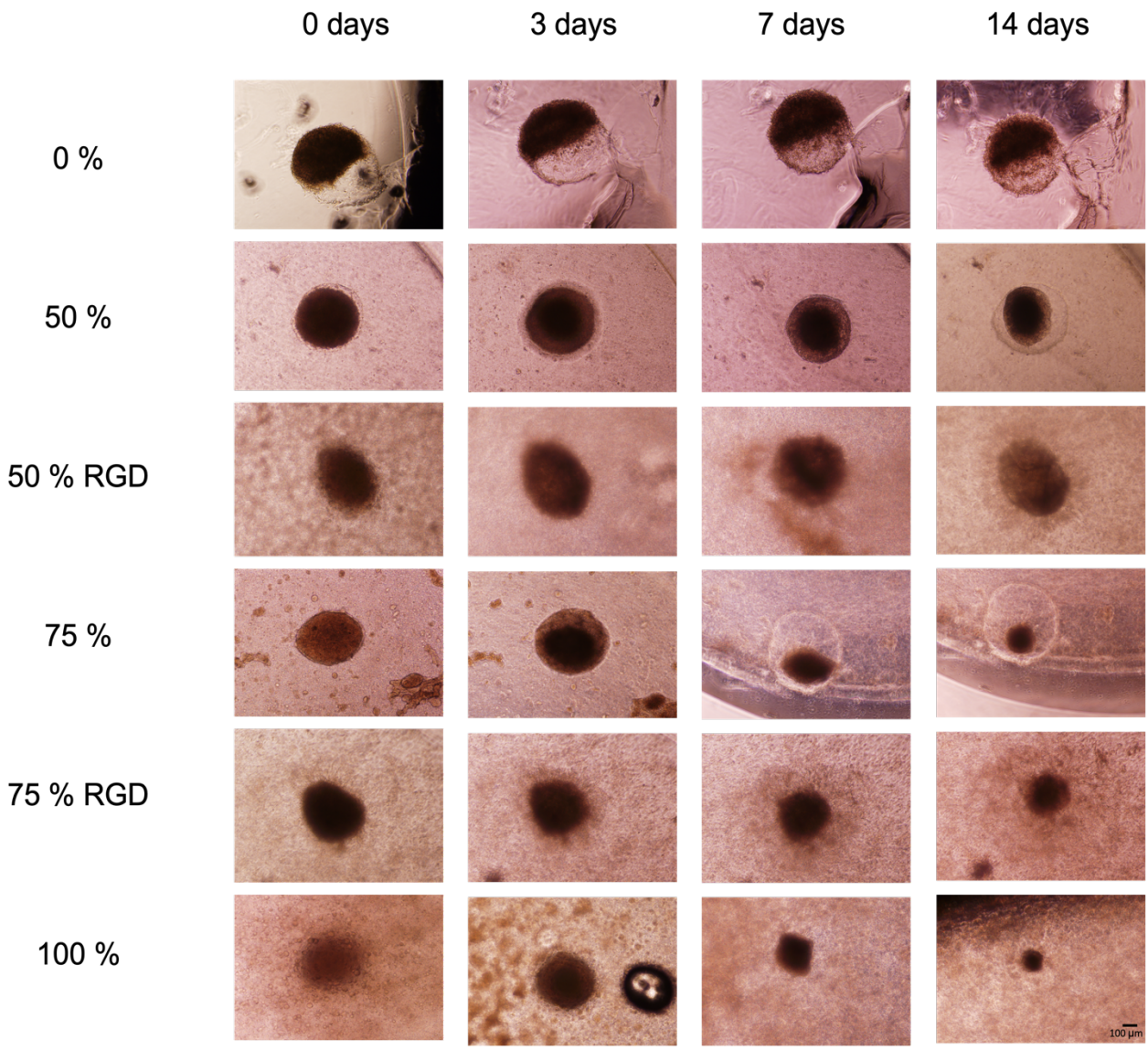

***Figure 3**: Representative phase contrast images of cell spheroids within the hydrogel samples with different PL concentrations with or without RGD. Observed at different timepoints: 0, 3, 7 and 14 days.*

4.3 Confocal imaging

Confocal laser scanning microscopy images show the extent of infiltration/invasion by immunolabelling of the nuclei (green) and the actin cytoskeleton (red). The invasion varied among the different samples. Figures 4 to 7 give a qualitative assessment of cells chemotaxis into the hydrogel matrix to visualize the extent of invasion of the cells.

Hydrogels with 75% PL without RGD show a more concentrated and condensed actin cytoskeleton on the Figure 6C compared to the 50% PL sample without RGD. On the other hand, the 0% PL sample shows no sign of invasion in Figure 4 as there is no sign of outgrowths from the spheroid. The 100% PL sample also shows no sign of outgrowth as seen in Figure 7.

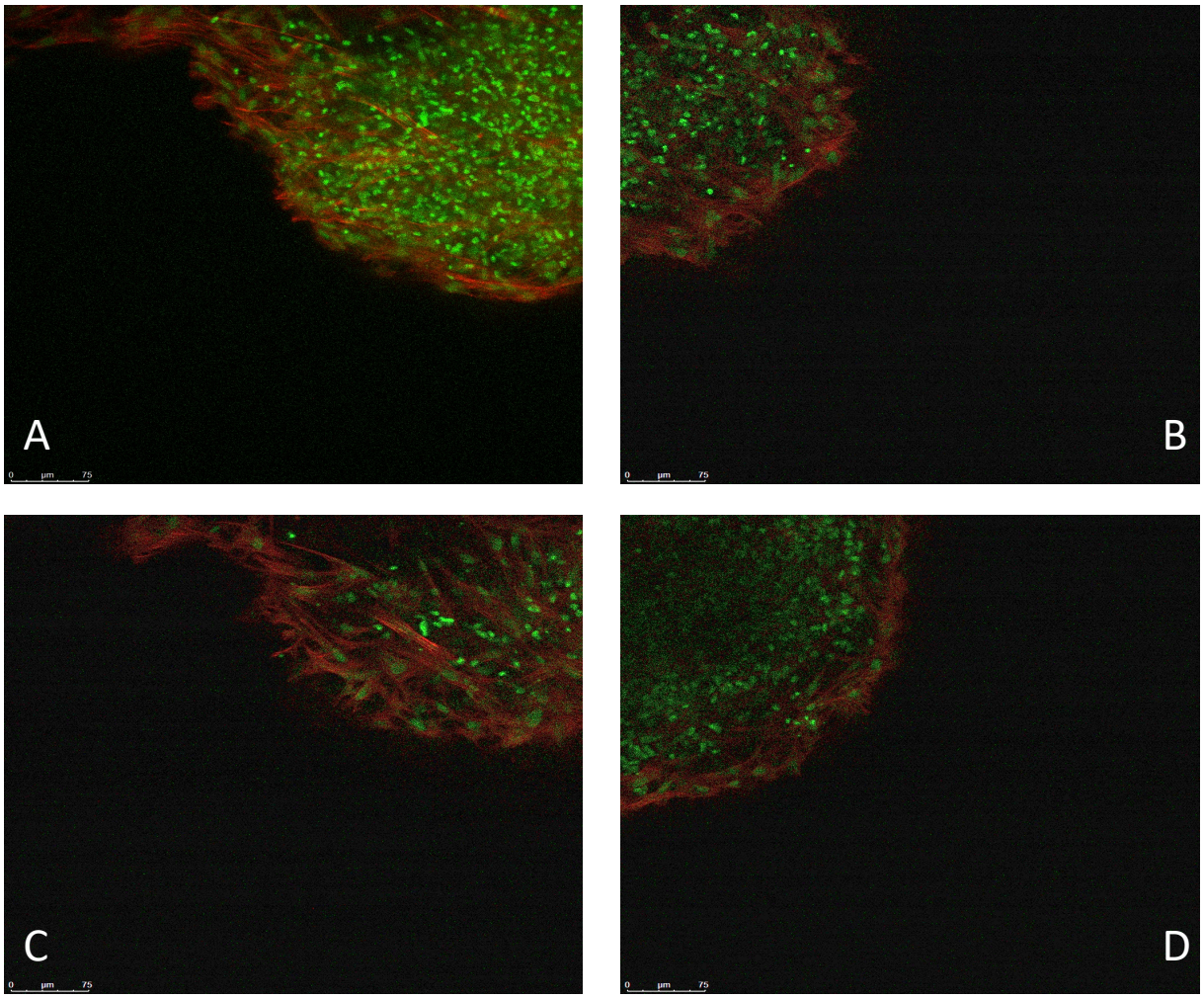

Figure 4: *CLSM images of 0% PL hydrogels, at 3 days. Immunolabeling of nuclei (green) and actin cytoskeleton (red). Scale bar represents 75µm.*

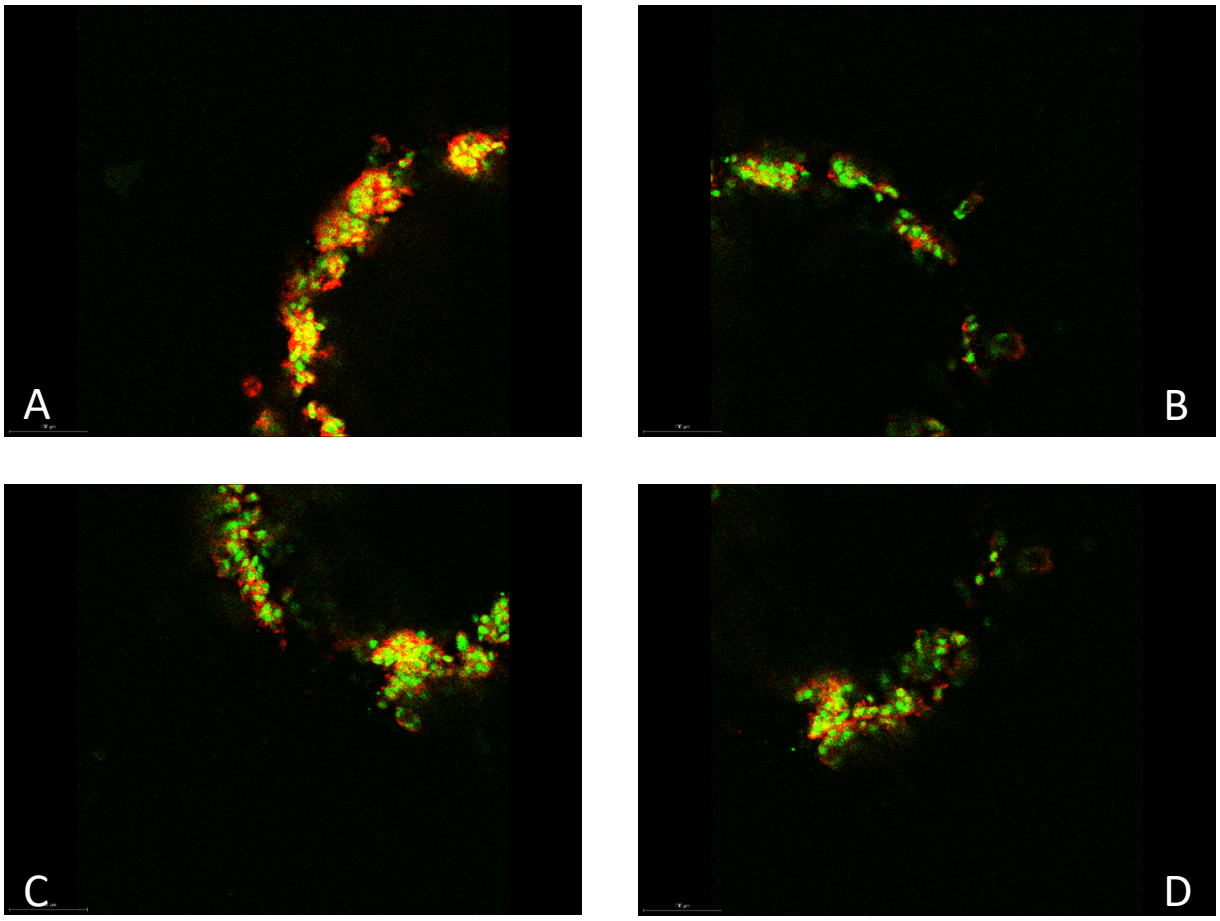

Figure 5*: CLSM images* of *50% PL hydrogels, at 3 days. Immunolabeling of nuclei (green) and actin cytoskeleton (red). Scale bar represents 100* µm.

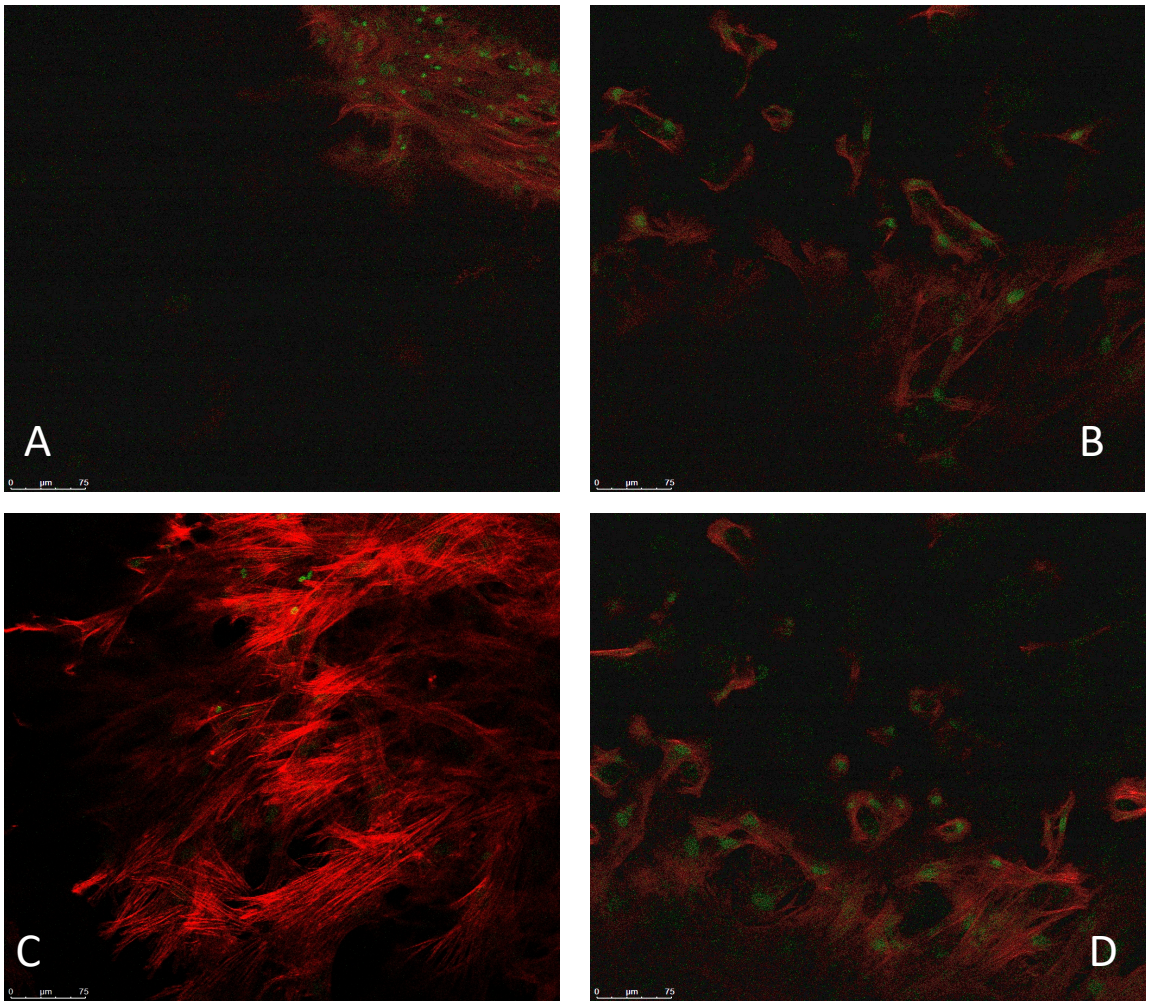

***Figure 6**: CLSM images of 75% PL hydrogels, at 3 days. Immunolabeling of nuclei (green) and actin cytoskeleton (red). Scalebar represents 75 µm.*

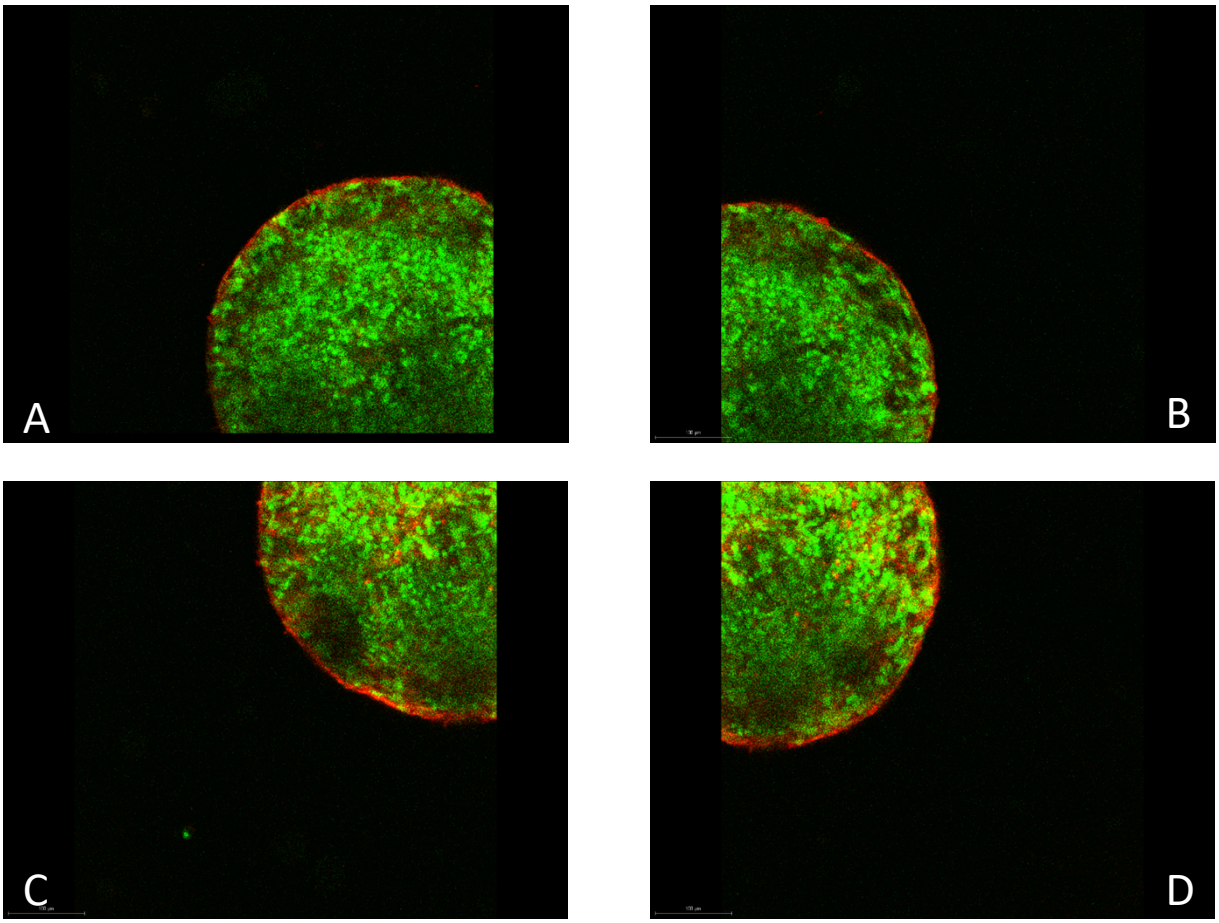

Figure 7: *CLSM images of 100% PL hydrogel, at 3 days. Immunolabeling of nuclei (green) and actin cytoskeleton (red). Scale bar represents 75 µm.*

5 Discussion

In this study we aimed of to investigate which concentration of platelet lysate proteins gives the best colonization of hydrogel matrix by hMSCs. In other words, we are trying to find the lowest amount of PL required for the sprouting of cells from encapsulated cell spheroids.

5.1 What does the BCA analysis tell us?

In all samples we observed a fast linear increase followed by a plateau, suggesting that the hydrogel has reached its maximum capacity for protein release. The initial increase in the graph can be explained as the rapid diffusion of proteins from the hydrogel to the surrounding environment. The rate of diffusion will then decrease as the total protein concertation decreases leading to the constant line after 24 h. This indicates the hydrogel has released as much protein as it can and has reached a point of equilibrium. This point where the rate of protein release is balanced by the rate of protein uptake or the remaining PL protein fraction is either physically or chemically entrapped within the PEG hydrogel matrix.

It was observed that at the protein release stops after 24 h for higher concentrations of 50%, 75% and 100%. However, with lower concentrations the protein release stops earlier. This gives us a better understanding of PL´s influence on the diffusivity of the hydrogel. These data suggest that hydrogels with higher PL concentrations will release more protein in a shorter time that hydrogels containing low concentrations. At higher platelet lysate concentrations, they can provide more growth factors and other bioactive molecules that promote protein release. The lower concentrations maintain their diffusion and have a more sustained release, due to less growth factors and other bioactive molecules that can be released from the hydrogel.

The diffusion kinetics can be interpreted from the BCA analysis. Comparing the slopes of the different PL concentrations, we can see that the lower PL concentrations have a lower slope of the release curve while the higher PL concentrations have higher slopes. A lower slope indicates a lower concentration gradient between the hydrogel and the external environment.

Ideally, it is preferred to produce a hydrogel with minimal swelling for periodontal regeneration [19]. Even though a rapid and high diffusion of protein is observed with higher PL concentrations, it can have its drawbacks. A higher PL concentration will

give a higher release of PL which gives more bioactivity. The higher bioactivity will lead to an increase in the swelling ratio of the hydrogels leading to a reduction in the gelation kinetics and higher chance of network imperfections [19].

This data is useful to understand the release kinetics of the hydrogel and for optimizing the design of the hydrogel to promote long term effectiveness of tissue generation. In addition, it can be used to interpret how much of the PL proteins remain in the hydrogel. The size of the proteins can play a role since some proteins can be too big to diffuse through the molecular network of the hydrogels thus influencing cell sprouting and colonization of the hydrogel [33, 34].

5.2 Is RGD necessary to facilitate cell sprouting in PL-loaded hydrogels?

The functionalization of hydrogels with RGD showed several observations of cell movement from the spheroid over time. As presented in the results section, cell migration is visible in hydrogels with 75% + RGD and 50% and RGD. Compared with the same concentrations that are not functionalized with RGD, there is no movement of cells in hydrogels that are not functionalized with RGD.

PL does promote cell migration on its own, but it did not provide sufficient amount of cell adhesion sites on its own as cells were not able to break out from the spheroid in the 100% PL hydrogel not functionalized with RGD unlike previously reported by Chahal et al. for adipose tissue-derived mesenchymal stem cells [19]. This goes against the hypothesis of this experiment since it was hypothesized increasingly more cell outgrowth would be observed with higher PL concentrations. This can be due to not centrifugation the PL prior to incorporating it to the hydrogels which can affect the amount of fibrinogen found in PL. Removing fibrinogen and clotted fibrin from the PL suspension reduces the amount of proteins that provide adhesion sites for cells in hydrogels not functionalized with RGD. On the other hand, the presence of fibrinogen can potentially inhibit cell outgrowth by forming fibrin networks which can trap growth factors [35, 36]. In addition, RGD on its own also does not provide enough stimulation to promote cell movement out from the spheroid as seen in the results above with the 0% PL which contained RGD without PL.

The cell movement observation in hydrogels with RGD suggest that this peptide assist in cell adhesion and migration. This can be explained by looking at the molecular components of the cells and RGD. Cells contain integrin receptors on their surface

[37]. These integrin receptors interact with the RGD peptide when they come in contact with the hydrogel. This interaction will then promote attachment of spreading cells.

Platelet lysates release a variety of growth factors and cytokines, however hydrogels with only PL show no sign of cell movement. This suggests that the bioactive molecules in PL can assist cell migration to an extent. While RGD promotes migration by interacting with integrin receptors, PL has a different mechanism. The active biomolecules in PL, such as growth factors can activate receptors on the surface of the cells that take part in cytoskeletal rearrangement and migration [38]. These receptors initiate intracellular signaling pathways that stimulate migration components such as actin filaments. Other bioactive molecules found in PL are chemokines such as CCL2, CCL3, IL-8 and PDGF, which influence stem cell migration [39, 40].

Even though RGD is observed to be vital for cell migration in this experiment, PL is also needed for enhancing tissue repair and regeneration. This is due to PL containing molecules such as chemotactic factors, cytokines and growth factors. A growth factor found in PL is transforming growth factor-beta (TGF- β) that stimulates osteoblast and fibroblast activity [30]. In addition, PL exerts chemotactic factors that have the effect to attract cells to the site of tissue injury or regeneration [41]. In all, this can increase the efficacy of hydrogels functionalized with RGD.

6 Conclusions

In conclusion, this experiment studied the effects of PL concentration and RGD on the behavior of the cells in the hydrogel.

The hypothesis in this experiment was that human MSCs encapsulated in PEG hydrogels sprout out from a cell spheroid and colonize the hydrogel matrix faster and more efficiently in hydrogels with higher platelet lysate concentration. The higher the PL concertation, the more effective the cell colonization. In this experiment, it was observed that cell colonization is visible with higher PL concentration, however the RGD peptide is essential. The findings suggest that the combination of PL and RGD in hydrogels have the potential to be an effective assist in cell migration. However, it is difficult to give any firm conclusions, further investigations should be done. Further studies need to be done to find the optimal design and to study the long-term effects of such treatment.

References

1. Scheuber, S., S. Hicklin, and U. Brägger, *Implants versus short-span fixed bridges: survival, complications, patients' benefits. A systematic review on economic aspects.* Clin Oral Implants Res, 2012. **23 Suppl 6**: p. 50-62.
2. Abraham, C.M., *A brief historical perspective on dental implants, their surface coatings and treatments.* Open Dent J, 2014. **8**: p. 50-5.
3. Mohajerani, H., et al., *The Risk Factors in Early Failure of Dental Implants: a Retrospective Study.* J Dent (Shiraz), 2017. **18**(4): p. 298-303.
4. Ata-Ali, J., et al., *Peri-implantitis: associated microbiota and treatment.* Med Oral Patol Oral Cir Bucal, 2011. **16**(7): p. e937-43.
5. Prathapachandran, J. and N. Suresh, *Management of peri-implantitis.* Dent Res J (Isfahan), 2012. **9**(5): p. 516-521.
6. Diaz, P., et al., *What is the prevalence of peri-implantitis? A systematic review and meta-analysis.* BMC oral health, 2022. **22**(1): p. 1-449.
7. Lindhe, J., et al., *Experimental breakdown of peri-implant and periodontal tissues. A study in the beagle dog.* Clin Oral Implants Res, 1992. **3**(1): p. 9-16.
8. Fürst, M.M., et al., *Bacterial colonization immediately after installation on oral titanium implants.* Clin Oral Implants Res, 2007. **18**(4): p. 501-8.
9. Kumar, A., et al., *Comparison of clinical and microbiological status of osseointegrated dental implant with natural tooth.* Journal of dental implants, 2017. **7**(2).
10. Wang, C., G. Fu, and F. Deng, *Difference of natural teeth and implant-supported restoration: A comparison of bone remodeling simulations.* Journal of Dental Sciences, 2015. **10**(2): p. 190-200.
11. Higaki, N., et al., *Do sensation differences exist between dental implants and natural teeth?: a meta-analysis.* Clin Oral Implants Res, 2014. **25**(11): p. 1307-1310.
12. Meyer, G., J. Fanghänel, and P. Proff, *Morphofunctional aspects of dental implants.* Annals of Anatomy - Anatomischer Anzeiger, 2012. **194**(2): p. 190-194.
13. Mohamed, J.B., et al., *The management of retrograde peri-implantitis: A case report.* J Clin Diagn Res, 2012. **6**(9): p. 1600-1602.
14. Romandini, M., et al., *Clinical signs, symptoms, perceptions, and impact on quality of life in patients suffering from peri-implant diseases: a university-representative cross-sectional study.* Clin Oral Implants Res, 2021. **32**(1): p. 100-111.
15. Dos Santos Martins, B.G., et al., *Surgical and Nonsurgical Treatment Protocols for Peri-implantitis: An Overview of Systematic Reviews.* Int J Oral Maxillofac Implants, 2022. **37**(4): p. 660-676.
16. Ting, M., et al., *Peri-implantitis: A Comprehensive Overview of Systematic Reviews.* J Oral Implantol, 2018. **44**(3): p. 225-247.
17. Mahato, N., X. Wu, and L. Wang, *Management of peri-implantitis: a systematic review, 2010-2015.* Springerplus, 2016. **5**: p. 105.
18. Rokaya, D., et al., *Peri-implantitis Update: Risk Indicators, Diagnosis, and Treatment.* Eur J Dent, 2020. **14**(4): p. 672-682.
19. Chahal, A.S., et al., *Human Platelet Lysate-Loaded Poly(ethylene glycol) Hydrogels Induce Stem Cell Chemotaxis In Vitro.* Biomacromolecules, 2021. **22**(8): p. 3486-3496.
20. Nicolas, J., et al., *3D Extracellular Matrix Mimics: Fundamental Concepts and Role of Materials Chemistry to Influence Stem Cell Fate.* Biomacromolecules, 2020. **21**(6): p. 1968-1994.

21. Karamanos, N.K., et al., *A guide to the composition and functions of the extracellular matrix.* Febs j, 2021. **288**(24): p. 6850-6912.
22. Lutolf, M.P. and J.A. Hubbell, *Synthetic biomaterials as instructive extracellular microenvironments for morphogenesis in tissue engineering.* Nature Biotechnology, 2005. **23**(1): p. 47-55.
23. Hubbell, J.A., *Bioactive biomaterials.* Current Opinion in Biotechnology, 1999. **10**(2): p. 123-129.
24. Lee, K.Y. and D.J. Mooney, *Hydrogels for Tissue Engineering.* Chemical Reviews, 2001. **101**(7): p. 1869-1880.
25. Arnaout, M.A., B. Mahalingam, and J.P. Xiong, *Integrin structure, allostery, and bidirectional signaling.* Annu Rev Cell Dev Biol, 2005. **21**: p. 381-410.
26. Hersel, U., C. Dahmen, and H. Kessler, *RGD modified polymers: biomaterials for stimulated cell adhesion and beyond.* Biomaterials, 2003. **24**(24): p. 4385-415.
27. Bellis, S.L., *Advantages of RGD peptides for directing cell association with biomaterials.* Biomaterials, 2011. **32**(18): p. 4205-10.
28. Xu, J., et al., *Platelet-rich plasma and regenerative dentistry.* Aust Dent J, 2020. **65**(2): p. 131-142.
29. Fortunato, T.M., et al., *Platelet lysate gel and endothelial progenitors stimulate microvascular network formation in vitro: tissue engineering implications.* Scientific Reports, 2016. **6**(1): p. 25326.
30. Babo, P.S., R.L. Reis, and M.E. Gomes, *Periodontal tissue engineering: current strategies and the role of platelet rich hemoderivatives.* J Mater Chem B, 2017. **5**(2): p. 3617-3628.
31. Maynard, D.M., et al., *Proteomic analysis of platelet alpha-granules using mass spectrometry.* J Thromb Haemost, 2007. **5**(9): p. 1945-55.
32. Chahal, A.S., et al., *Attachment and spatial organisation of human mesenchymal stem cells on poly(ethylene glycol) hydrogels.* J Mech Behav Biomed Mater, 2018. **84**: p. 46-53.
33. Deuel, T.F. and J.S. Huang, *Platelet-derived growth factor. Structure, function, and roles in normal and transformed cells.* J Clin Invest, 1984. **74**(3): p. 669-676.
34. Pillarisetti, K. and S.K. Gupta, *Cloning and relative expression analysis of rat stromal cell derived factor-1 (SDF-1)1: SDF-1 alpha mRNA is selectively induced in rat model of myocardial infarction.* Inflammation, 2001. **25**(5): p. 293-300.
35. Maynard, D.M., et al., *Proteomic analysis of platelet α-granules using mass spectrometry.* Journal of Thrombosis and Haemostasis, 2007. **5**(9): p. 1945-1955.
36. Baek, S.J., S.K. Kang, and J.C. Ra, *In vitro migration capacity of human adipose tissue-derived mesenchymal stem cells reflects their expression of receptors for chemokines and growth factors.* Exp Mol Med, 2011. **43**(10): p. 596-603.
37. Docheva, D., et al., *Human mesenchymal stem cells in contact with their environment: surface characteristics and the integrin system.* J Cell Mol Med, 2007. **11**(1): p. 21-38.
38. Yu, D.-M., et al., *The molecular mechanism of platelet lysate promotes transformation of non-union cells into osteoblasts.* Transl Cancer Res, 2020. **9**(3): p. 1985-1992.
39. Anitua, E., et al., *Autologous platelets as a source of proteins for healing and tissue regeneration.* Thromb Haemost, 2004. **91**(1): p. 4-15.

40. Mendes, B.B., et al., *Blood derivatives awaken in regenerative medicine strategies to modulate wound healing.* Adv Drug Deliv Rev, 2018. **129**: p. 376-393.
41. Burnouf, T., et al., *Human platelet lysate: Replacing fetal bovine serum as a gold standard for human cell propagation?* Biomaterials, 2016. **76**: p. 371-87.

Appendix

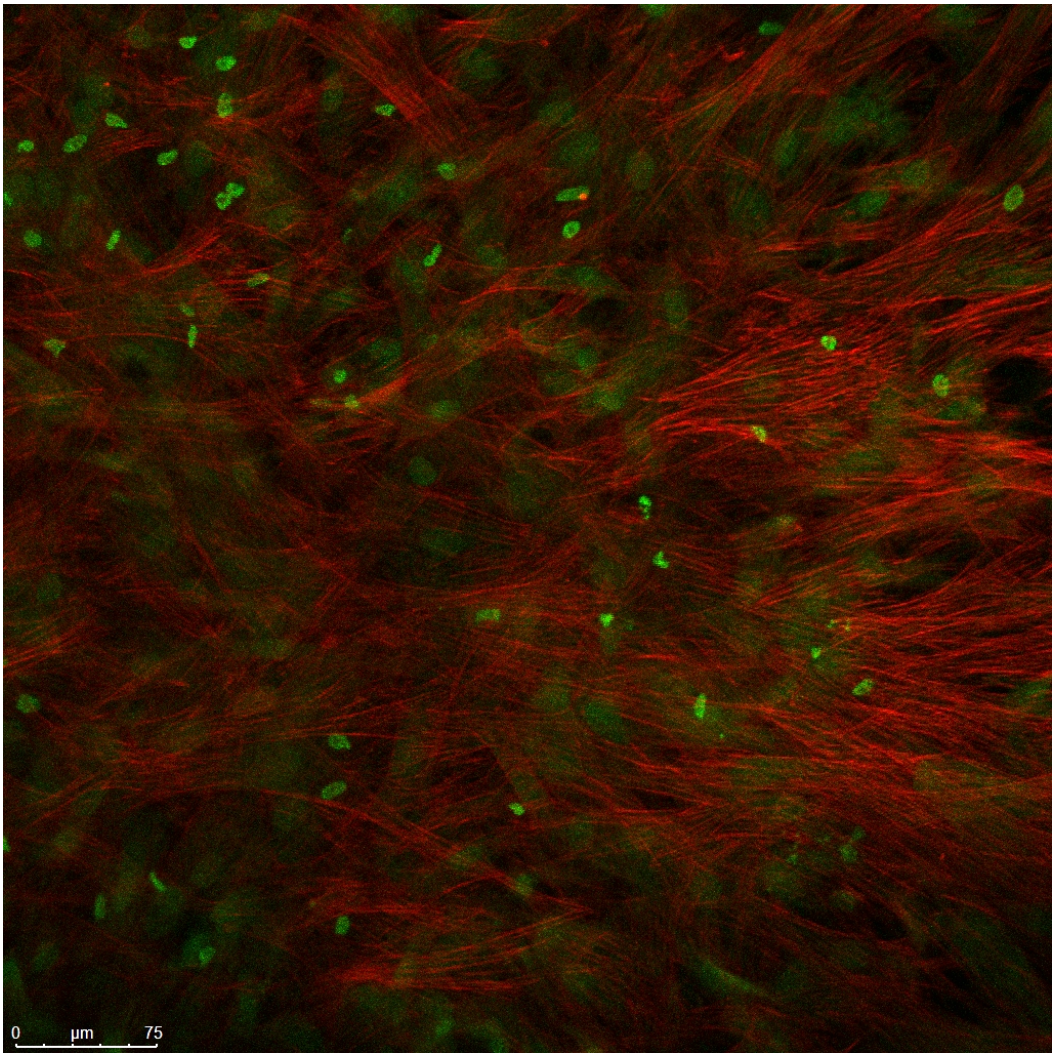

***Appendix 1**: CLSM images of 75% functionalized with RGD. Immunolabeling of nuclei (green) and actin cytoskeleton (red).*

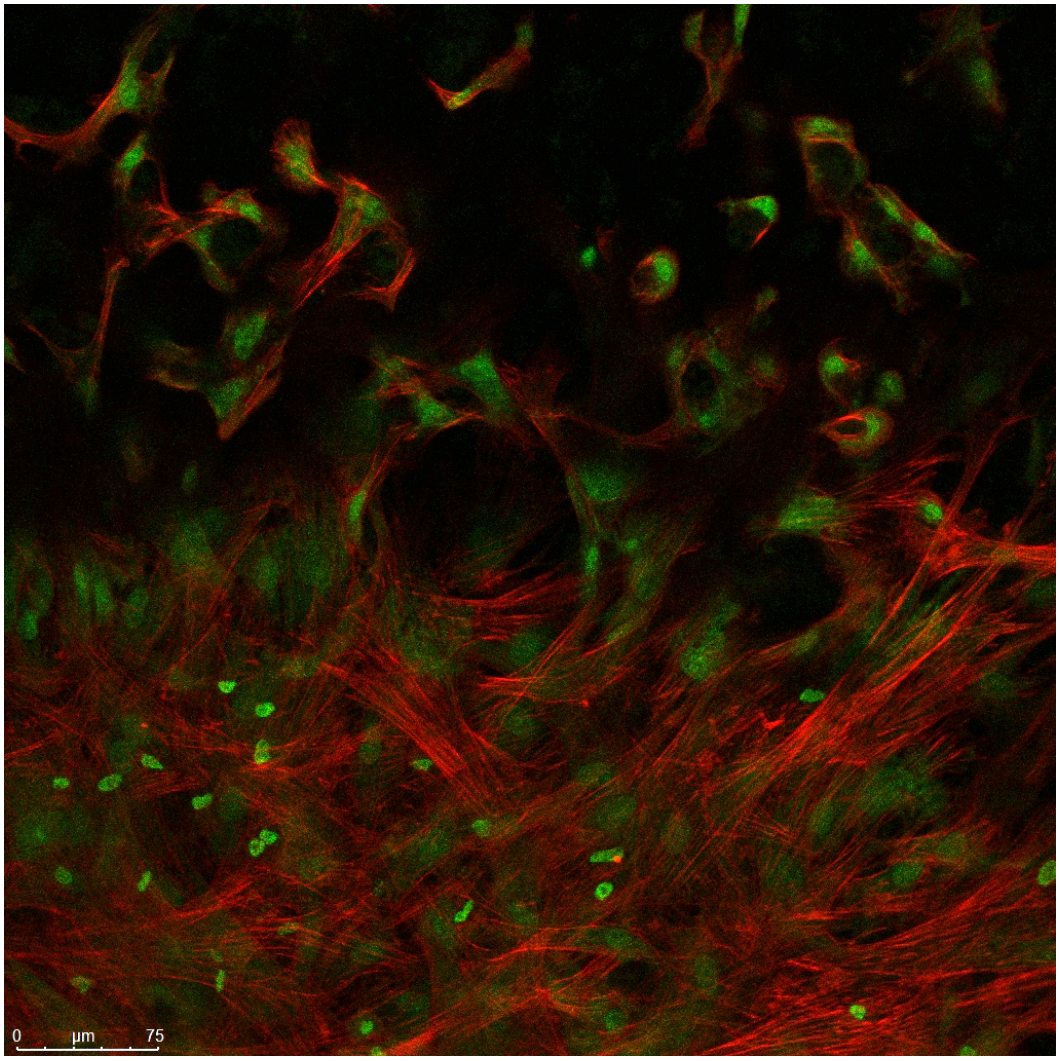

***Appendix 2**: CLSM image of 75% functionalized with RGD. Immunolabeling of nuclei (green) and actin cytoskeleton (red).*